アカデミックプログラム［B講演］ | 09. 錯体化学・有機金属化学：口頭B講演

2025年3月29日(土) 9:00 ~ 11:40 [B]A301(第2学舎 1号館 [3階] A301)

[[B]A301-4am] 09. 錯体化学・有機金属化学

座長：桑田 繁樹、二瓶 雅之

英語
9:00 ~ 9:20
[[B]A301-4am-01]
ホフマン型金属有機構造体におけるFe(II)スピンクロスオーバーのCO_2駆動制御

○高坂 亘[1]、Abhik PAUL[2]、Bhart KUMAR[2]、Dibya MONDAL[2]、Sanjit KONAR[2]、宮坂 等[1] (1. 東北大学、2. インド科学教育研究大学)

英語
9:20 ~ 9:40
[[B]A301-4am-02]
キラル配位子を用いた立体異性鉄(II)錯体のスピンクロスオーバー温度と分子間相互作用の関係

○高野 莉奈[1]、Ay Burak[2]、石田 尚行[1] (1. 電気通信大学、2. チュクロワ大学)

英語
9:40 ~ 10:00
[[B]A301-4am-03]
2-Dimensional Image Data Analysis of Color Dynamics in Electrochromic Display Devices

○Shifa Sarkar[1,2], Takefumi Yoshida[3], Masayoshi Higuchi[1,2] (1. Osaka University, 2. National Institute for Materials Science (NIMS), 3. Wakayama University)

英語
10:00 ~ 10:20
[[B]A301-4am-04]
Magnetic Interplay in Spin-intercalated Hybrid Layered Magnets

○Qingxin Liu[1,2], Honoka Nemoto[1,2], Haruka Yoshino[1,2], Wataru Kosaka[1,2], Hitoshi Miyasaka[1,2] (1. Department of Chemistry, Graduate School of Science, Tohoku University, 2. Division of Solid-State Metal-Complex Chemistry, IMR, Tohoku University)

英語
10:20 ~ 10:40
[[B]A301-4am-05]
立方体型[Mo_3S_4Fe]クラスターによるCO_2からCH_4への触媒的変換

○松岡 優音[1]、Sameera W. M. C.[2]、谷藤 一樹[1]、大木 靖弘[1] (1. 京大化研、2. ゴセンバーグ大)

英語
10:40 ~ 11:00
[[B]A301-4am-06]
Cp系配位子を有する立方体型[$Mo_nM_{4-n}S_4$]クラスターによるCO_2還元 (M = Fe; n = 2) およびC-Hボリル化反応 (M = Rh, Ir; n = 3)

○下山 さやか[1]、松岡 優音[1]、伊豆 仁[1]、谷藤 一樹[1]、大木 靖弘[1] (1. 京都大学化学研究所)

英語
11:00 ~ 11:20
[[B]A301-4am-07]

環状鉄ビスシリル骨格を基軸とする脱酸素反応

○菅 雄翔[1]、砂田 祐輔[1,2] (1. 東大院工、2. 東大生研)

英語

11:20 ~ 11:40

[[B]A301-4am-08]

P^{t}Bu$_3$で保護された正二十面体型鉄55核ヒドリドクラスターの合成

○田中 奏多[1]、大石 峻也[2]、川本 晃希[2]、唯 美津木[2]、W.M.C Sameera[3]、高畑 遼[1]、寺西 利治[1]、吉川 聡一[4]、山添 誠司[4]、志賀 拓也[5]、二瓶 雅之[5]、加藤 立久[6]、Roger E. Cramer[7]、Zihan Zhang[8]、Karsten Meyer[8]、伊豆 仁[1]、檜垣 達也[1]、大木 靖弘[1] (1. 京大化研、2. 名大院理・名大物質国際研、3. Dept of Chem. & Mol. Biol., Univ. of Gothenburg、4. 都立大理、5. 筑波大院数物、6. 京大福井センター、7. Dept of Chem., Univ. of Hawaii、8. Dept of Chem. & Pharm., FAU Erlangen-Nürnberg)

CO_2-actuated Control of Fe(II) Spin Crossover in a Hofmann-type Metal-Organic Framework

([1]*Institute for Materials Research, Tohoku University*, [2]*Department of Chemistry, Indian Institute of Science Education and Reserach*) ○Wataru Kosaka,[1] Abhik Paul,[2] Bhart Kumar,[2] Dibya Jyoti Mondal,[2] Hitoshi Miyasaka,[1] Sanjit Konar[2]

Keywords: Metal−Organic Framework; Spin Crossover; Gas-responsive magnetic property; Gas Adsorption; Carbon dioxide

The increased anthropogenic emission level of CO_2 urges the development of CO_2-responsive materials, but is it possible to regulate the inherent electronic properties through weak physisorption of a ubiquitous gas such as CO_2? Herein, we intended to answer this imperative question by the first case of CO_2-actuated variable spin-state stabilization in an interdigitated Hofmann-type metal-organic framework $[Fe^{II}Pd(CN)_4L_2]$ (**1**, L = methyl isonicotinate) [1].

Compound **1** did not adsorb N_2 (77 K) and O_2 (90 K). In contrast, a sharp transition appeared in the CO_2 adsorption isotherm and isobar, indicating the occurrence of gated adsorption. Magnetic measurements were conducted using a home-built gas cell under an external magnetic field of 1 kOe and varied CO_2 pressure (Fig. 1a), showing a wide shift in transition temperature ($T_{1/2}$) from 178 K at P_{CO2} = 0 kPa to 229 K at P_{CO2} = 100 kPa (defined by the average of cooling and heating). Interestingly, the emergence of a stepped behavior in the heating process below P_{CO2} = 10 kPa and overlapping magnetic susceptibility values above P_{CO2} = 10 kPa elucidate the selective low-spin state stabilization correlated with the extent of CO_2 accommodation. Based on the magnetic response and phase transition diagrams obtained under respective P_{CO2} (Fig. 1b), a plausible scenario of the spin-state switching can be interpreted as [**1**(ls) + **1**'(ls)] → [**1**(hs) + **1**'(ls)] → **1**(hs) at $P_{CO2} \leq$ 10 kPa, **1**'(ls) → **1**(hs) at 10 kPa < $P_{CO2} \leq$ 32 kPa, and **1**'(ls) → **1**'(hs) → **1**(hs) at P_{CO2} = 100 kPa, where **1** and **1**' represent CO_2-free and CO_2-accommodated states, respectively. The cooperative CO_2 adsorption with spin transition based on the varied CO_2 pressure corroborates a novel case for developing CO_2-responsive magnetic materials.

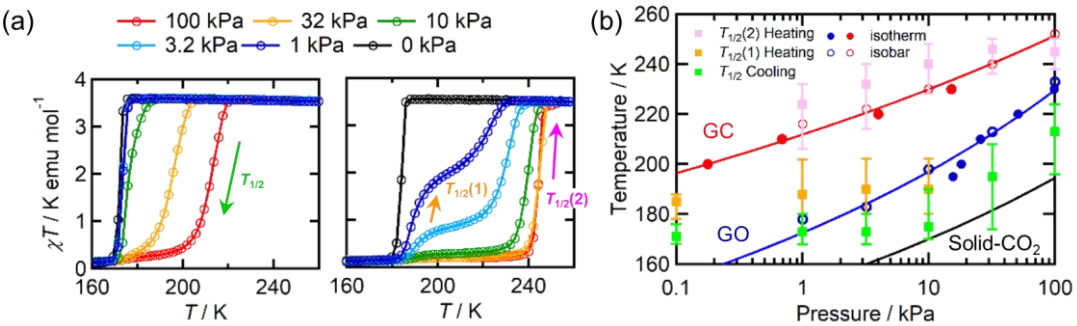

Fig. 1 (a) χT-T plots under CO_2 on cooling (right) and heating (right). (b) T-P phase diagram

1) A. Paul, W. Kosaka, B. Kumar, D. J. Mondal, H. Miyasaka, S. Konar, *Chem. Sci.* **2024**, *15*, 15610.

Effects of Intermolecular Interactions on the SCO Temperature in Stereoisomeric Iron(II) Complexes with Chiral Ligands

(1*The University of Electro-Communications*, 2*Çukurova Üniversitesi*) ○Rina Takano[1], Ay Burak[2], Takayuki Ishida[1]

Keywords: Spin Crossover; Stereochemistry; Magnetic Properties; Crystal Structure

Complexes $[FeL^{R}_2(NCS)_2]$ (L = 2-pyridylmethyleneamino-R) are well known to exhibit spin crossover (SCO).[1] We investigate the influence of stereoisomerism on SCO properties[2] and prepared several types of stereoisomeric SCO complexes with ligands derived from racemic and enantiopure 1,2-dimethylpropylamine ($dmipNH_2$) and 2-pyridinecarboxaldehyde. These complexes exhibit various stereoisomers because the ligands induce *cis*/*trans* isomer and contain chiral centers, such as *R*/*S* in the ligands and *Δ*/*Λ* in the iron(II) center.

The selective synthesis can be controlled by the starting material and complexation temperature. Single crystal structure analysis was performed on all products to determine their stereostructure (Fig. a). Each material exhibits different magnetic properties for example HS, half-SCO, and full-SCO (Fig. b). According to van't Hoff analysis, $T_{1/2}$ and $\Delta_{tr}H$ are corelated, indicating that the SCO behaviors seem to be enthalpy-driven. Since the intramolecular Fe-N_6 electronic environments are similar to each other, it becomes significantly important how to define and measure intermolecular as well as intramolecular steric effects. The results suggest a possible relationship between $T_{1/2}$ and the percentage of N···H-C contacts on Hirshfeld surface[3] (Fig. c), which indicates that N···H-C contacts with neighboring molecules stabilize the HS state.

(a) (b) (c)

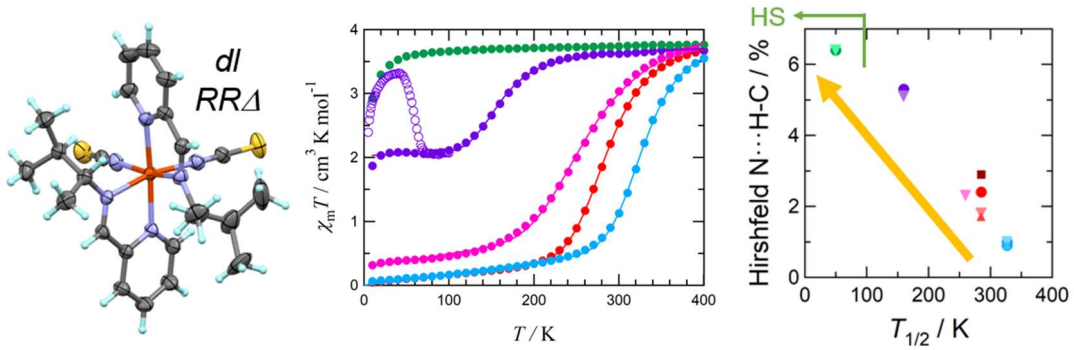

Figure (a) Ortep drawing of $[FeL^{dmip}_2(NCS)_2]$. (b) χ_mT vs T plots for **half-SCO$_{rac}$** (purple), **full-SCO$_{rac1}$** (pink), **full-SCO$_{rac2}$** (red), **HS$_R$** (green), and **full-SCO$_R$** (turquoise). (c) The relation between percentage of N···H-C contact from Hirshfeld analysis and SCO temperature.

[1] N. Mochida et al., *Magnetochemistry* **2020**, *1*, 17. [2] M. Oppermann et al., *Nat. Chem*. **2022**, *14*, 739. [3] P. R. Spackman et al., *J. Appl. Cryst*., **2021**, *54*, 1006.

2-Dimensional Image Data Analysis of Color Dynamics in Electrochromic Display Devices

([1]*Graduate School of Information Science and Technology*, *Osaka University*, [2]*National Institute for Materials Science,* [3]*Wakayama University*) ○Shifa Sarkar,[1,2] Takefumi Yoshida,[3] Masayoshi Higuchi[1,2]

Keywords: Electrochromic Devices; Image Data Analysis; Metallosupramolecular Polymer

Electrochromic devices (ECDs) represent advanced innovations that employ voltage-responsive materials capable of altering color, making them ideal for diverse applications like display devices, smart windows, and energy-saving systems.[1] Among electrochromic (EC) materials, metallo-supramolecular polymers (MSPs) have gained significant interest because of their inherent structural versatility and adjustable optical properties.[2] However, a major challenge lies in the analytical methods used to examine their EC characteristics. Traditional methods, which typically depend on spectrophotometric techniques, often lack sufficient spatial resolution and are incapable of capturing the complete dynamic range of EC transitions.[3]

We report a two-dimensional (2D) image-based analytical approach that combines high-resolution imaging with quantitative analysis to overcome these shortcomings. A solid-state polyFe-based ECD was fabricated using a spray coating method. A non-uniform color change from purple to colorless was observed in the ECD. A movie of the EC changes was taken during the cyclic operation at 1.2 V. Images were extracted from the movie then converted to grayscale images, from where pixel values were extracted using Python OpenCV. Finally, a contrast versus time graph was generated using the pixel values to analyze the EC transition pattern across the entire device (Fig. 1). This analysis revealed that the reaction time in the device became slower in the central region compared to the edge regions due to the variations in localized resistances within the ITO electrodes.

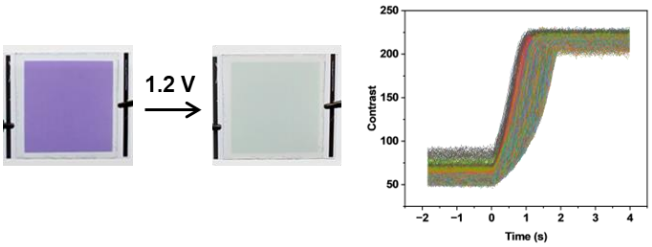

Fig. 1: Color-changing pattern of polyFe-based ECD.

ACKNOWLEDGMENT: this research was supported by the Mirai project (JPMJMI21I4) from the Japan Science and Technology Agency (JST) and the Environment Research and Technology Development Fund (JPMEERF20221M02) from Environmental Restoration and Conservation Agency (ERCA).

1) Higuchi, M.; J. Mater. Chem. C **2014**, *2*, 9341. 2) Gustavsen, A.; Sol. Energy Mater. Sol. Cells, **2010**, *94*, 105. 3) Higuchi, M.; Sol. Energy Mater. Sol. Cells, **2019**, *200*, 110000.

Guest-induced Reversible Transition of Visible-Hidden Frustration Behavior in Spin-intercalated Hybrid Layered Magnets

([1]*Graduate School of Science, Tohoku University*, [2]*Institute for Materials Research, Tohoku University*) ○Qingxin Liu,[1,2] Honoka Nemoto,[1,2] Haruka Yoshino,[1,2] Wataru Kosaka,[1,2] Hitoshi Miyasaka[1,2]

Keywords: Reversible transition; Spin frustration; Hybrid magnets

Chemo-responsive magnetism is a desired function in molecular magnets for potential applications in memory, sensors, and switches. However, it is challenging to achieve drastic, large, and highly reversible functions in such materials. Recently, we constructed a type of spin-intercalated hybrid layered magnet, where the magnetic interplay determines the bulky magnetism of hybrids and induces some interesting magnetic behavior.[1-3] For example, a new frustrated phase was isolated due to the competitive magnetic interactions,[2] and dynamic spin reordering was realized under the internal magnetic fields generated by the ferrimagnetic layers.[3] Nevertheless, the reversible change of magnetic properties in hybrid magnets induced by guest ad-/desorption has not been reported so far. Here, a reversible change between visible and "hidden" spin frustrated state was demonstrated in spin-intercalated hybrid magnets, $[FeCp^*_2]\{[Ru_2(2,3,5\text{-}F_3PhCO_2)_4]_2(TCNQ)\}\bullet n$DCE ($n$ = 2, **2-DCE**; n = 0, **2**; $2,3,5\text{-}F_3PhCO_2^-$ = 2,3,5-trifluorobenzoate, TCNQ = 7,7,8,8-tetracyano-*p*-quinodimethane; DCE = 1,2-dichloroethane), via ad-/desorption of solvent molecules (Fig. 1a and 1b).

Compound **2** was obtained by evacuating **2-DCE** at 353 K for 12 h. The electronic state of both **2-DCE** and **2** were the same, represented as $[FeCp^*_2]^+[\{Ru_2^{II,II}\}_2(TCNQ^{\bullet-})]$. In magnetic measurement, a spin frustrated (FR) phase was observed in **2-DCE** (visible FR, Fig. 1e) due to the magnetic competition between interlayer (J_{NNNI}) and $[FeCp^*_2]^+$–$TCNQ^{\bullet-}$ (J_{NNI}) interactions (Fig. 1c). However, the FR behavior was suppressed in **2** (Fig. 1e), which may be due to the stronger J_{NNI} than J_{NNNI} (Fig. 1d), showing a seemingly ferrimagnetic (F) behavior ("hidden" FR). Namely, we successfully switched the visible and hidden FR behavior reversibly by guest ad-/desorption (Fig 1e) in this hybrid layered magnet.

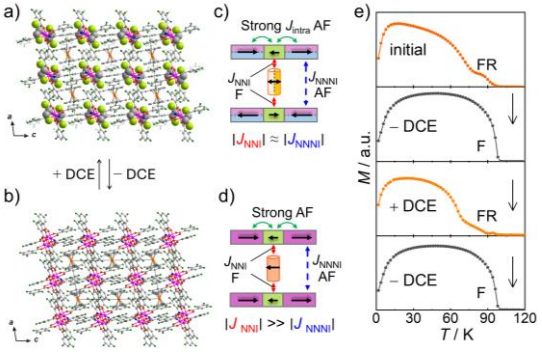

Fig. 1 Packing views along *b*-axis and proposed spin configuration of **2-DCE** (a, c) and **2** (b, d), respectively. e) FCM curves at H_{dc} = 10 Oe under ad-/desorption of DCE vapor.

1) H. Fukunaga, *et al*., *Angew. Chem.*, **2015**, *127*, 579. 2) H. Fukunaga, *et al*., *Chem. Eur. J.*, **2020**, *26*, 16755. 3) Q. Liu, *et al*., *Chem. Sci*., **2024**,*15*, 19411.

CO_2 to CH_4 reduction catalyzed by a [Mo_3S_4Fe] cluster

([1]*Institute for Chemical Research, Kyoto University*, [2] *Department of Chemistry and Molecular Biology, University of Gothenburg*) ○Yuto Matsuoka,[1] W. M. C. Sameera,[2] Kazuki Tanifuji,[1] Ohki Yasuhiro[1]

Keywords: Metal-sulfur cluster; CO_2 reduction; CH_4 formation; Molecular catalyst

Transition metal-sulfur (M-S) clusters in some enzymes are known to catalyze reductions of inert small molecules such as N_2 and CO_2.[1,2] Our group aimed to mimic such catalytic functions of the biological clusters and reported catalytic silylation of N_2 by a bio-inspired cubic M-S cluster, [Cp*$_3$$Mo_3S_4$FeCl] (**1**, Cp* = C_5Me_5, Figure A).[3] Strong interactions between the Cp* ligand and the Mo atoms suppress undesirable aggregation of the cluster and determine the substrate binding site as the Fe center. The unusual stability of cluster **1** suggested a better catalytic performance in CO_2 reduction than previously reported for M-S clusters.[4] Herein, we report catalytic CO_2 reduction to CH_4 by **1**, which is more efficient and productive than reported for the M-S clusters.

Catalytic reactions were performed under CO_2 (1 atm) in the presence of SmI_2 and H_2O as an electron and proton source. A reaction run with cluster **1** as a catalyst exhibited the formation of CH_4 (230 ± 18 equiv. per catalyst) with 37% selectivity based on SmI_2. Most of the remaining SmI_2 was consumed for H_2 generation (1396 ± 48 equiv. with 56% selectivity). The reaction did not terminate due to the inactivation of the catalyst, as the higher loading of SmI_2 improved the turnover number of the CH_4 formation to 2062 equiv. Interestingly, the concurrent formation of CO, a typical product of CO_2 reduction, was at the substoichiometric level of the catalyst.

A plot of produced CH_4 amount vs. reaction time shows the completion of the reaction within 30 min and the absence of an induction period (Figure B). The maximum turnover frequencies (TOFs) of the CH_4 and H_2 production reached 8.4 ± 0.7 and 148 ± 41 min^{-1}, respectively. In addition, initial CH_4 formation rates displayed a linear relationship with catalyst concentrations (Figure C), suggesting that **1** catalyzes the CH_4 formation from CO_2 as the single catalyst molecule rather than nanoparticles or aggregates.

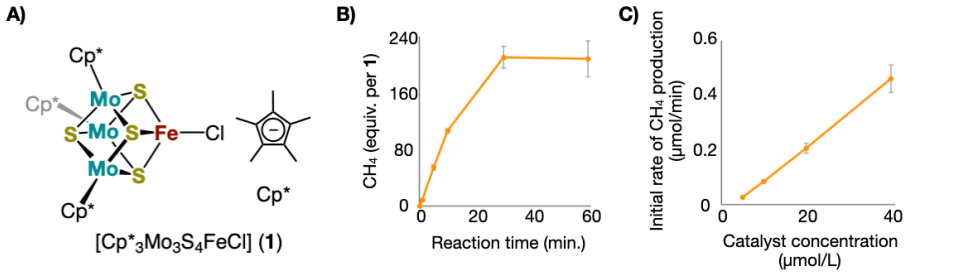

1) T. Spatzal *et al*. *Science* **2011**, *334*, 940. 2) J. Fesseler *et al*. *Angew. Chem. Int. Ed.* **2015**, *54*, 8560. 3) Y. Ohki *et al*. *Nature* **2022**, *607*, 86. 4) For example, see: K. Tanifuji *et al*. *Angew. Chem. Int. Ed.* **2016**, *55*, 15633.

Applications of cuboidal $[Mo_nM_{4-n}S_4]$ clusters with Cp-type ligands for CO_2 reduction (M = Fe; n = 2) and C-H borylation (M = Rh, Ir; n = 3)

(*ICR, Kyoto U.*) ○Sayaka Shimoyama, Yuto Matsuoka, Hitoshi Izu, Kazuki Tanifuji, Yasuhiro Ohki

Keywords: *multinuclear complex, metal-sulfur cluster; molecular catalyst, CO_2 reduction, C-H borylation*

Transition metal-sulfur clusters catalyze reductions of inert small molecules as enzymatic cofactors. FeMoco ([(*R*-homocitrate)$MoFe_7S_9C$]) is the catalytic active site of nitrogenase and reduces inert small molecules, such as N_2 and CO_2.[1] We have synthesized $[Cp^R{}_3Mo_3FeS_4Cl]$ (**1**) ($Cp^R = Cp^{XL}$ ($C_5Me_4SiEt_3$), Cp* (C_5Me_5)) as structural and functional analogs of FeMoco,[2] which catalyze N_2 [3] and CO_2 reduction. In this work, we targeted the following two reactions to expand the utility of this catalyst framework: (i) CO_2 reduction by a cluster with two Fe sites and (ii) conversion of hydrocarbons by clusters containing 4d or 5d transition metal as a reaction site.

A cuboidal cluster with two Fe sites, $[Cp^{XL}{}_2Mo_2Fe_2S_4Cl_2]$ (**2**), was synthesized for the first topic. Treatment of $Cp^{XL}MoCl_4$ with 4 eq. of LiS^tBu and 1 eq. of $FeCl_3$ gave **2** in 21% yield as suggested from the literature procedure for the Cp* analog.[4] Cluster **2** was characterized through X-ray and electrochemical analyses. The catalytic evaluation for the CO_2 reduction revealed that **2** exhibits CH_4 formation from CO_2 with higher turnover frequency than cluster **1** which contains a single Fe site.

The study for the second topic focused on the synthesis of cuboidal $[Mo_3MS_4]$ clusters, $[Cp^R{}_3Mo_3MS_4L]$ ($Cp^R = Cp^{XL}$, Cp*; M = Rh, Ir; L = cod, coe), and the development of their catalytic activity for C-H borylation. Corresponding to the synthetic procedure for cluster **1**,[2] $Cp^R{}_3Mo_3S_4$ was treated with 1.2 eq. of KC_8 and 1 eq. of Rh or Ir complex ($[RhCl(cod)]_2$, $[RhCl(coe)_2]_2$, $[IrCl(coe)_2]_2$) to give respective $[Mo_3MS_4]$ clusters in 31-40% yield. The clusters were characterized through ^{1}H NMR and X-ray analyses. All synthesized clusters catalyzed the C-H borylation of aromatic compounds (benzene, toluene, *o*-xylene, *m*-xylene, and *p*-xylene) as the first example in synthetic metal-sulfur clusters. The best conversion yield was achieved by $[Cp^*{}_3Mo_3RhS_4(coe)]$ in any case, probably due to its less hindered reaction site and higher reactivity of Rh than Ir to the substrates.

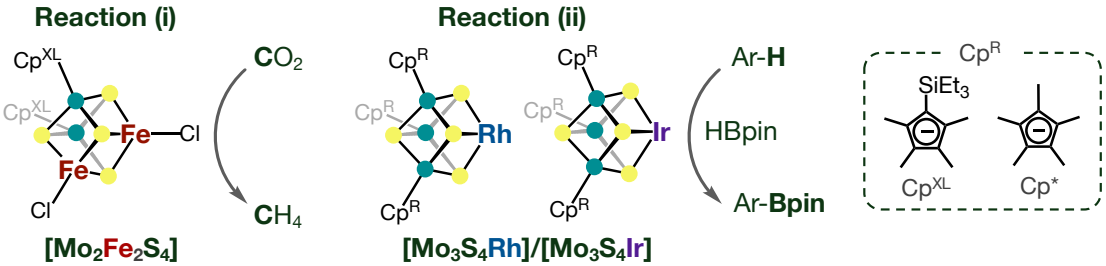

1) Jasniewski, A. J.; Lee, C. C.; Ribbe, M. W.; Hu, Y. *Chem. Rev.* **2020**, *120*, 5107-5157. 2) Ohki, Y. *et al*. *Inorg. Chem.* **2019**, *58*, 5230-5240. 3) Ohki, Y. *et al*. *Nature* **2022**, *607*, 86-90. 4) Kawaguchi, H.; Yamada, K.; Ohnishi, S.; Tatsumi, K. *J. Am. Chem. Soc.* **1997**, *119*, 10871-10872.

Deoxygenation Reactions Enabled by Cyclic Bis(silyl)iron Skeletons as Key Fragments

([1]*Graduate School of Engineering and* [2]*Institute of Industrial Science, The University of Tokyo*)
○Yuto Suga[1], Yusuke Sunada[1,2]

Keywords: Iron, Silicon, Deoxygenation, Carbene

Organosilyl ligands attached to the transition-metal centers exhibit unique reactivities, especially toward oxygen-containing substrates owing to their electropositivities. For instance, when a carbonyl compound reacts with a transition-metal-silyl complex, a siloxyalkyl complex is formed via insertion of the C=O double bond to the metal−silicon bond (Scheme 1-a).[1] Furthermore, it was reported by several research groups that transition-metal-disilyl complex could give rise to the formation of a transition-metal-carbene intermediate by treatment with a carbonyl compound via intramolecular deoxygenation from the siloxyalkyl complex formed as stated above (Scheme 1-b).[2] Although this type of reaction is expected as a new synthetic route of transition-metal-carbene complexes, the isolation of the transition-metal-carbene intermediates has not been reported, instead, the formation of them was confirmed by trapping experiments in the previous reports. Inspired by these precedented works, we decided to elucidate the mechanism of the deoxygenation reaction to obtain better understandings of the reactivity of organosilicon-based ligands attached to the transition metal centers, as well as to establish a new synthetic method of transition-metal-carbene complexes.

We found that iron complexes **1** and **2** bearing chelating disilyl ligands (Chart 1) reacted with aryl aldehydes to afford corresponding stilbene derivatives in a deoxygenative manner. Moreover, when **1** was reacted with cyclopropenone derivatives, iron-cyclopropenylidene complexes were formed, which are the first examples of structurally determined transition-metal-carbene complexes generated via deoxygenation reaction induced by transition-metal-disilyl complexes. The proposed mechanism of the deoxygenation reaction will be presented based on the isolation of various iron complexes formed in the deoxygenation reaction.

Scheme 1.

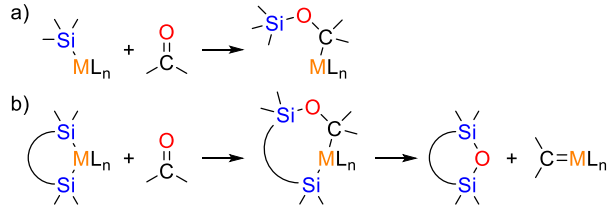

Chart 1.

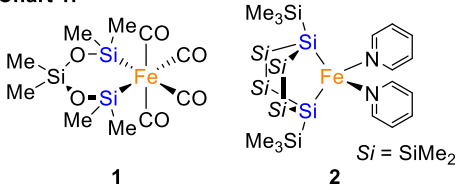

1 **2**

[1] M. T. Whited, B. L. H. Taylor, *Comments Inorg. Chem.* **2020**, *40*, 217.
[2] (*a*) D. L. Johnson and J. A. Gladysz, *J. Am. Chem. Soc.* **1979**, *101*, 6433; (*b*) H. Nakazawa, D. L. Johnson and J. A. Gladysz, *Organometallics* **1983**, *2*, 1846; (*c*) J. Barrau, N. Ben Hamida, H. Agrebi and J. Satge, *Inorg. Chem.* **1990**, *29*, 1674; (*d*) J. Barrau and N. B. Hamida, *Inorganica Chim. Acta* **1990**, 175, 159; (*e*) J. Barrau and N. B. Hamida, *Inorganica Chim. Acta* **1990**, *178*, 141; (*f*) M. Ishikawa, A. Naka, S. Okazaki and H. Sakamoto, *Organometallics* **1993**, *12*, 87; (*g*) A. Naka, K. K. Lee, K. Yoshizawa, T. Yamabe and M. Ishikawa, *Organometallics* **1999**, *18*, 4524; (*h*) Y. Kang, S. O. Kang and J. Ko, *Organometallics* **2000**, *19*, 1216.

An Icosahedral 55-Atom Iron Hydride Cluster Protected by Tri-*tert*-butylphosphines

([1]*Institute for Chemical Research, Kyoto Univ.*, [2]*Graduate School of Science and RCMS, Nagoya Univ.*, [3]*Dept of Chem. & Mol. Biol., Univ. of Gothenburg*, [4]*Graduate School of Science, Tokyo Metropolitan Univ.*, [5]*Dept of Chem., Univ. of Tsukuba*, [6]*Fukui Institute for Fundamental Chemistry*, [7]*Dept of Chem., Univ. of Hawaii*, [8]*Dept of Chem. & Pharm., FAU Erlangen-Nürnberg*) ○Kanata Tanaka,[1] Shunya Oishi,[2] Koki Kawamoto,[2] Mizuki Tada,[2] W. M. C Sameera,[3] Ryo Takahata,[1] Toshiharu Teranishi,[1] Soichi Kikkawa,[4] Seiji Yamazoe,[4] Takuya Shiga,[5] Masayuki Nihei,[5] Tatsuhisa Kato,[6] Roger E. Cramer,[7] Zihan Zhang,[8] Karsten Meyer,[8] Hitoshi Izu,[1] Tatsuya Higaki,[1] Yasuhiro Ohki[1]

Keywords: Cluster; Crystal Structure; Hydride; XAFS

Nanoclusters are nanometer-sized molecular compounds characterized by significant metal–metal bonding and low average oxidation states, and they exhibit unique properties distinct from those of small metal complexes or nanoparticles.[1)] In contrast to the diverse range of sizes and structures discovered for coinage metal nanoclusters, the family of iron clusters remains limited to the subnanometer scale (i.e., <1 nm)[2)3)] owing to the relatively weak iron–iron bonds and the high reactivity of low oxidation state iron. Here, we report the characterization of a cationic 55-atom Fe nanocluster paired with an anionic 6-atom Fe cluster, formulated as $[Fe_{55}H_{46}(P^tBu_3)_{12}][Fe_6H_8\{N(SiMe_3)_2\}_6]$ (**[Fe$_{55}$][Fe$_6$]**)[4)].

[Fe$_{55}$][Fe$_6$] was synthesized from the reaction of $Fe\{N(SiMe_3)_2\}_2$ with HBpin in the presence of bulky P^tBu_3 in 13% yield. Single-crystal X-ray crystallography confirmed the structure of **[Fe$_{55}$][Fe$_6$]**. **[Fe$_{55}$]** has an icosahedral core with a diameter of 1.2 nm and the 12 vertices of the **Fe$_{55}$** icosahedron are occupied by P^tBu_3 ligands. In contrast, **[Fe$_6$]** displays an octahedral core with each Fe atom bound to a silylamide (i.e., $-N(SiMe_3)_2$) (Figure A). Electrospray ionization (ESI) mass spectrometric analysis was performed to determine the formulas, including the hydrides, of the **[Fe$_{55}$]** cation and the **[Fe$_6$]** anion. X-ray absorption fine structure (XAFS) analysis determined the average oxidation state of Fe in **[Fe$_{55}$][Fe$_6$]** (Figure C). Further characterization of **[Fe$_{55}$][Fe$_6$]** was carried out using other analytical techniques.

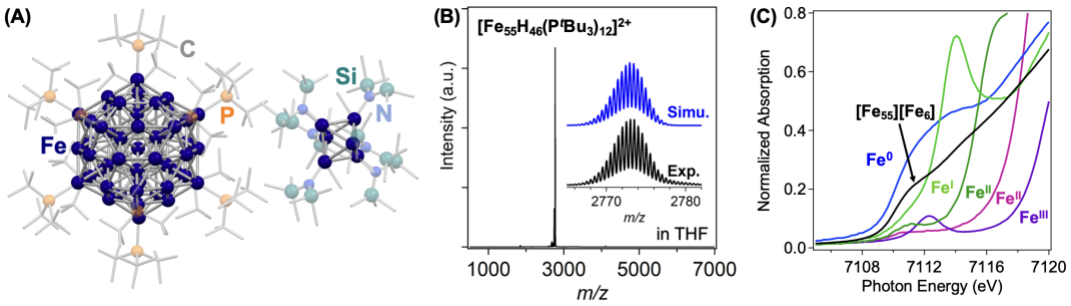

Figure. (A) Crystal structure, (B) Positive-mode ESI mass spectrum, and (C) Fe *K*-edge XANES spectrum of **[Fe$_{55}$][Fe$_6$]**. Reference samples for XAFS analysis: Fe^0 (blue) = Fe powder, Fe^I (light green) = $[K(18\text{-crown-}6)][Fe\{N(SiMe_3)_2\}_2]$, Fe^{II}(green) = $Fe\{N(SiMe_3)_2\}_2$, Fe^{II} (violet) = $FeCl_2$, Fe^{III} (purple) = $FeCl_3$.

1) Tsukuda, T.; Häkkinen, H. Protected Metal Clusters: From Fundamentals to Applications. Elsevier, **2015**. 2) Hayton, T. W. *Atomically Precise Nanochemistry* (eds Jin, R., Jiang, D.-E..) 285−307 (John Wiley & Sons Ltd., 2023). 3) Ohki, Y. *et al. J. Am. Chem. Soc.* **2017**, *139*, 5596-5606. 4) Ohki, Y. *et al. J. Am. Chem. Soc. in press.*